

Interaction hierarchy among Cdv proteins drives recruitment to membrane necks

Reviewed Preprint

v1 • January 16, 2025

Not revised

Nicola De Franceschi, Alberto Blanch-Jover, Cees Dekker 

Department of Bionanoscience, Kavli Institute of Nanoscience Delft, Delft University of Technology, Delft, The Netherlands • IMol Polish Academy of Sciences, Warsaw, Poland

 https://en.wikipedia.org/wiki/Open_access Copyright information

eLife Assessment

This **valuable** study investigates how the proteins of the Cdv division system in *Metallosphaera sedula* archaea sequentially interact with curved membranes *in vitro*, extending our understanding of this reduced ESCRT-like machinery. While the data support key aspects of protein recruitment and membrane remodeling, missing controls and statistical analysis information, unaddressed discrepancies, and limitations in recapitulating native geometry leave the data **incomplete** to fully support the proposed conclusions. The work will be of interest to evolutionary and synthetic biologists as membrane biophysicists but would benefit from additional experiments and a more cautious interpretation of results.

<https://doi.org/10.7554/eLife.104226.1.sa4>

Abstract

Cell division in the crenarchaea is accomplished by the Cdv system. In *Sulfolobus* cells, it was observed that an initial non-contractile ring of CdvA and CdvB forms at the mid location of the cell, which is followed by a second ring of CdvB1 and CdvB2 that appear to drive the constriction of the cell membrane. Here, we use an *in vitro* reconstituted system to explore how protein interactions among these Cdv proteins govern their recruitment to the membrane. We show that CdvA does not bind the membrane unless in complex with CdvB. We find that CdvB2 can polymerize if its self-inhibitory domain is removed, and that by itself it exhibits poor binding to the membrane. However, CdvB2 can be efficiently recruited to the membrane by both CdvB1 and CdvB. Furthermore, the CdvB1:CdvB2 co-polymer can be recruited to the membrane by CdvA:CdvB. By reconstituting these proteins in dumbbell-shaped liposomes, we show that Cdv proteins have a strong preference to localize at membrane necks of high curvature. Our findings clarify many of the mutual protein interactions of the Cdv system and their interaction with the membrane, thus helping to build a mechanistic understanding of cell division in archaeal cells.

Introduction

Cell division in the archaeal phylum of the crenarchaea is performed by the Cdv system (Lindås et al., 2008 [↗](#); Samson et al., 2008 [↗](#)). While this protein machinery is unique to archaea, some of its components are homologous to the ESCRT-III proteins that are responsible for the cell division, vesicle budding, and many other reverse-topology membrane-scission processes in eukaryotes (Schöneberg et al., 2016; Hurley, 2015 [↗](#)). This homology is one of the many similarities that eukaryotes share with archaea, which reinforces the widespread idea that these two kingdoms of life share an evolutionary root (Cox et al., 2008 [↗](#)).

Since the Cdv system was first described 15 years ago in *Sulfolobus sulfataricus*, it has been shown to be present in many other species of the TACK superphylum of archaea (Makarova et al., 2010 [↗](#)). It is composed of CdvA, the CdvB paralogs (homologous to ESCRT-III in eukaryotes), and CdvC (homologous to the eukaryotic Vps4) (Samson et al., 2008 [↗](#)). The first cell imaging of the Cdv system showed a ring of CdvA and CdvB forming at the center of the cell between two segregated nucleoids during division, which over time colocalized with a ring of CdvC in the same position (Lindås et al., 2008 [↗](#)). All these 3 proteins are located in the same operon (Lindås et al., 2008 [↗](#)), while paralogs of CdvB (namely CdvB1, CdvB2 and CdvB3) are located in other parts of the genome. Recently, it was reported that these paralogs play a crucial role in cell division (Tarrason Risa et al., 2020 [↗](#)). A recent model for cell division in crenarchaea is that CdvA and CdvB initially form a ring at the centre of the cell, where it subsequently recruits CdvB1 and CdvB2 (Tarrason Risa et al., 2020 [↗](#)). At this point, CdvB is digested by the proteasome and the initial CdvA:CdvB ring gets removed from the membrane, while CdvB1 and CdvB2 are left to perform the constriction of the membrane, presumably through the interaction of CdvB1 directly with the membrane (Blanch Jover et al., 2022 [↗](#)), until the final step of scission (Tarrason Risa et al., 2020 [↗](#)). CdvC is a AAA ATPase that has been suggested to remove monomers of CdvB1 and CdvB2 from the ring, generating a turnover that ensures cellular constriction while avoiding steric hindrance at the neck (Tarrason Risa et al., 2020 [↗](#); Harker-Kirschneck et al., 2022 [↗](#)). This model of action of the Cdv proteins is supported by some experimental findings on live cells. When generating mutant cells of *S. sulfataricus* lacking CdvB1, these presented a normal constriction of the membrane, but some cells failed to perform the last step of scission, leaving them with two full copies of the genome (Pulschen et al., 2020 [↗](#)). Furthermore, cells lacking CdvB2 were able to perform the scission normally, but tended to present a misplacement of the constricting ring, resulting in aberrant daughter cells that were not equally sized (Pulschen et al., 2020 [↗](#)). This indicates that the two paralogs responsible for the constriction actually perform different roles during the division process. However, it also shows how cells with any of these two proteins can still perform, albeit with difficulties, the full process of constriction and scission on their own.

While a global picture has thus been emerging, many of the underlying mechanistic interactions remain unclear. CdvA has an E3B domain (ESCRT-III binding region; see **Figure 1A** [↗](#)) through which it is capable of interacting with the wH (winged helix) region of CdvB (Moriscot et al., 2011 [↗](#)). None of the other paralogs present such a wH domain (Caspi et al., 2018). Additionally, CdvA can bind to lipid membranes while CdvB is not able to do so (Samson et al., 2011 [↗](#)). Therefore, CdvA is seen as the membrane recruiter of CdvB to the membrane. In turn, CdvB is known to interact with CdvB1, which then interacts with CdvB2 (Samson et al., 2008 [↗](#)), suggesting that CdvB is the recruiter of the CdvB1:CdvB2 constricting ring. Finally, during the constriction of the membrane, CdvC is presumed to disassemble the filaments of the CdvB1:CdvB2 polymer to generate a turnover of protein and thus supply energy to the system to deform the membrane (Harker-kirschneck et al., 2022 [↗](#)). This ATPase features major structural similarities to the eukaryotic Vps4 (Caillat et al., 2015 [↗](#)), which is known to be responsible for the depolymerization of ESCRT-III filaments (Lata et al., 2008 [↗](#); Azad et al., 2023 [↗](#)) and to create a turnover of ESCRT-III components at the membrane (Chiaruttini et al., 2015 [↗](#); Pfitzner et al., 2020). In archaea, this

similarity is further strengthened by *in vitro* experiments where CdvC was able to depolymerize CdvB1 filaments and detach CdvB1 from lipid membranes into solution (Blanch Jover et al., 2022 [↗](#)).

Little is yet known about how the Cdv proteins are hierarchically recruited to the membrane and how their mutual interactions affect this process. Here, we explore these questions using a bottom-up reconstitution approach. We find that CdvA can bind to lipid membranes only when it is interacting with CdvB, but not on its own. We observe that CdvB2 can be recruited to the membrane by both CdvB1 and CdvB. Finally, we show that all Cdv proteins exhibit a preferential binding for highly curved membranes and preferentially localize at the necks of dumbbell-shaped vesicles.

Results

Filament formation by CdvA

Previous *in vitro* studies of purified CdvA were done with either a full-length version of the protein from *M. sedula* (Moriscot et al., 2011 [↗](#)) or with an N-terminus-truncated CdvA from *S. acidocaldarius* that was missing the initial PRC barrel (**Figure 1A** [↗](#)) (Samson et al., 2011 [↗](#); Dobro et al., 2013 [↗](#)). The phenotype of these two versions differed in that the full-length protein formed double helical filaments that were reported to be stabilized by the binding of DNA, whereas the N-terminus-truncated CdvA did not polymerize. At the same time, the N-terminus-truncated CdvA was shown to be able to bind to lipid membranes and recruit CdvB to the membrane along with it. For our study, we purified full length CdvA from *M. sedula*, following the protocol published by Moriscot et al., 2011 [↗](#), and we obtained the same type of filaments as described in their work (Supplementary Figure 1A). However, we never observed interaction between CdvA and lipid membranes (data not shown). We then decided to fuse the full length CdvA to an MBP-tag. The resulting purified MBP-CdvA formed short and thick polymers (Supplementary Figure 1B), which had an average length of 90 ± 40 nm (mean \pm SD, N=195) and a width of 12 ± 3 nm (mean \pm SD, N=156). When treating the protein with a TEV protease that cleaved the MBP from the protein, CdvA polymerized into long and thin filaments (**Figure 1B** [↗](#)) with an average length of 220 ± 100 nm (mean \pm SD, N=102) and a width of 5 ± 1 nm (mean \pm SD, N=106). Formation of these filaments did not require addition of DNA. Thus, the presence of the MBP tag allowed to control the polymerization of CdvA.

CdvB recruits CdvA to membrane necks

Next, we sought to investigate the lipid-binding capabilities of the full-length CdvA. For this, we used a liposome flotation assay, where protein was mixed with negatively charged Small Unilamellar Vesicles (SUVs) (see Methods), added to a sucrose gradient, and spun at high speed. This yielded multiple fractions: upper fraction(s) containing liposomes (1), intermediate fraction(s) containing the soluble unbound protein, and the bottom fraction containing protein filaments sedimented at the bottom of the tube. In these assays, we mixed MBP-CdvA with the lipids together with TEV protease, in order to cleave the MBP tag. When testing for the binding of CdvA to lipid membrane, we observed that the protein was always found in both the soluble and the filamented fractions, but never bound to lipids (**Figure 1C** [↗](#)). We then purified CdvB which, as previously shown (Moriscot et al., 2011 [↗](#)), presented no filamentation regardless of having the MBP-tag or not. When CdvA was mixed with CdvB, both proteins were found primarily in the liposome-bound fraction (**Figure 1C** [↗](#)). This indicates that the binding of full-length CdvA to the lipid membrane occurs only when in complex with CdvB.

The human ESCRT-III system preferentially locates at membrane necks that present high curvatures (De Franceschi et al., 2018 [↗](#); Bertin et al., 2020 [↗](#); Pfitzner et al., 2020 [↗](#)). We explored if a similar preference for high curvatures could be observed for Cdv proteins as well. Here, we

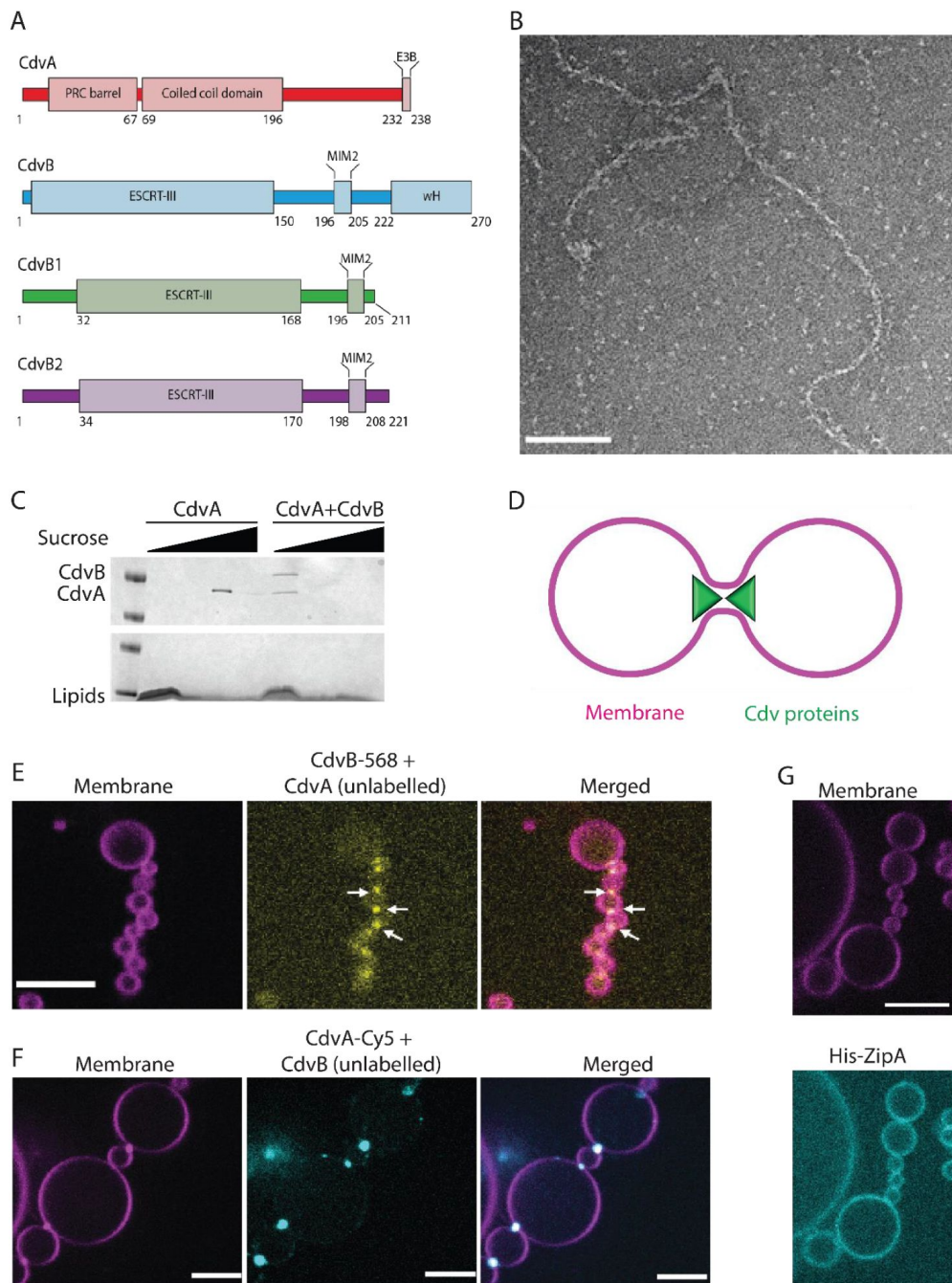


Figure 1

polymerization and membrane binding of the CdvA:CdvB complex

(A) Schematic depicting the domain architecture of Cdv proteins. **(B)** Negative staining TEM image of elongated filaments formed by CdvA upon removal of the MBP tag in the absence of DNA. Scale bar: 80 nm. **(C)** Coomassie staining of flotation assay. CdvA is found to not bind lipid membranes on its own (i.e. lane 1 is empty). However, in presence of CdvB, both proteins bind liposomes. **(D)** Schematic representing the topology of Cdv proteins reconstituted inside dumbbell-shaped liposomes, recapitulating the shape of a dividing cell. **(E)** Spinning disk confocal images of the CdvA:CdvB complex reconstituted inside dumbbell-shaped liposomes. CdvB is fluorescently labelled, CdvA is unlabelled. CdvB is observed to localize at the neck. **(F)** Same as panel e, but with fluorescently labelled CdvA and unlabelled CdvB. CdvA is observed to localize at the neck. **(G)** Binding of His-tagged ZipA to dumbbell liposomes containing 18:1 DGS-NTA lipids. As expected for a protein binding the membrane via a His-tag, ZipA exhibits a homogeneous membrane distribution, without enrichment at the neck. Scale bars: 10 μ m.

used a recently developed SMS approach to produce dumbbell-shaped liposomes (De Franceschi et al., 2022 [↗](#)). Briefly, a lipid mixture including negatively charged lipids in chloroform was dried out and resuspended in oil. In this oil, we formed water-in-oil droplets in which the proteins were encapsulated, and these droplets were then left to sedimented by gravity through a lipid interface into an outer water phase, thus obtaining unilamellar liposomes that contained the protein on the inside. The outer phase was made of buffer containing DNA “nanostars” that anchor to the membrane, inducing curvature thereby generating dumbbells. We thus obtain chains of dumbbell-shaped liposomes that are mutually connected through membrane necks. Protein that are encapsulated within these liposomes can be studied for their binding in a membrane geometry that resembles cells that are dividing (**Figure 1D** [↗](#)). Such a system was recently used to demonstrate a membrane scission activity of Dynamin A (De Franceschi et al., 2024 [↗](#)).

In these dumbbell-shaped liposomes, we observed a clear preference of the CdvA:CdvB complex to localize at the membrane necks (**Figure 1E, 1F** [↗](#)). Proteins displayed a strong fluorescence signal at the membrane necks, while they showed only a residual weak homogeneous binding to other membrane regions of the dumbbell-shaped liposomes. We also performed control experiments with a protein that bound the membrane via a His-tag (ZipA from *E. coli*) and that was not expected to sense curvature. As expected, ZipA did not show any significant enrichment of the protein signal at the necks (**Figure 1G** [↗](#) and Supplementary Figure 1C), indicating that the enrichment on highly curved membranes is a specific property of the Cdv proteins and not an artifact induced by the SMS assay.

Filaments formation by CdvB1 and CdvB2ΔC

Next, we purified CdvB2 from *M. sedula* fused to an MBP-tag. The resulting protein was not presenting any spontaneous filamentation either with or without the MBP tag (Supplementary Figure 2A, 2B). Moreover, we found that full-length CdvB2 was unable to bind membranes in liposome binding assays, neither alone nor in combination with CdvB1 (Supplementary Figure 2C). ESCRT-III proteins commonly feature an inactive soluble state and an active membrane-bound state (Tang et al., 2015 [↗](#)). Indeed, *in vitro*, these proteins remain inactive soluble monomers while they may get activated and able to polymerize by deleting their C-terminus part (Shim et al., 2007 [↗](#)). The same has been previously shown for purified CdvB (Moriscot et al., 2011 [↗](#)), which did not present any polymerization *in vitro*, but spontaneously assembled into filaments upon removal of its C-terminus. Hence, we decided to explore if the same was true for CdvB2, and we made a C-terminal truncated version that contained amino acids 1-170 of CdvB2, henceforth denoted as CdvB2ΔC.

TEM imaging of the CdvB2ΔC-MBP fusion protein showed that it was polymerizing into a characteristic shape of well-defined short linear filaments (Supplementary Figure 2D). The filaments had an average length of 166 ± 63 nm (mean \pm SD; N=161) and a width of 20 ± 5 nm (mean \pm SD; N=129). Similarly to CdvA, CdvB2ΔC assembled into longer and thinner filaments upon MBP tag cleavage (**Figure 2A** [↗](#) and Supplementary Figure 2E, 2F), of average length 245 ± 95 nm (mean \pm SD; N=36) and width of 14 ± 3 nm (mean \pm SD; N=64). These data indicate that CdvB2 also presents a self-inhibitory domain, and that filament formation can be triggered by its removal.

Since CdvB2 forms part of the constricting ring together with CdvB1, we explored the effects of their interaction on filament formation. When mixing CdvB1 and CdvB2ΔC together, filaments formed with a very similar length (272 ± 94 (mean \pm SD; N=84)) and width (15 ± 6 (mean \pm SD; N=184)) to that of CdvB2ΔC alone (**Figure 2B** [↗](#) and Supplementary Figure 2E, 2F). Interestingly, these filaments appeared to be more curved. To quantify this, we measured the ratio of the end-to-end distance to the contour length of filaments, which equals 1 for perfectly straight filaments but is <1 for curved ones. For CdvB2ΔC filaments we measured a ratio of 0.86 ± 0.13 , while the CdvB1:CdvB2ΔC co-polymer yielded a ratio of 0.75 ± 0.21 (**Figure 2C** [↗](#)). This may also imply that the CdvB1:CdvB2ΔC copolymer is more flexible than the CdvB2ΔC homopolymer.

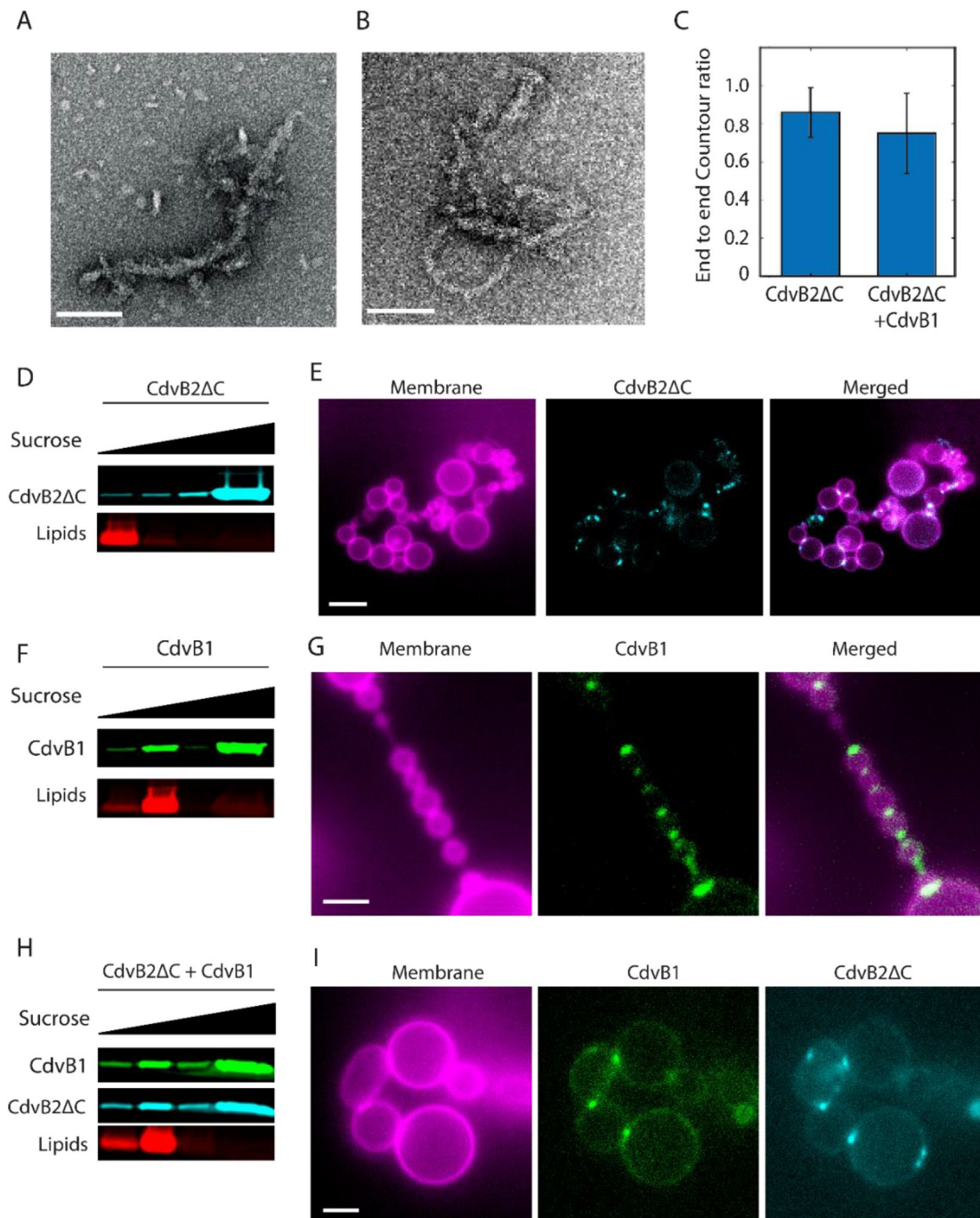


Figure 2

polymerization and membrane binding of the CDVB1: CdvB2ΔC complex.

(A) Negative staining TEM image of CdvB2ΔC filaments obtained upon removal of the MBP tag. **(B)** Negative staining TEM image of CdvB1:CdvB2ΔC co-polymer. Scale bars: 100 nm. **(C)** Ratio of the end-to-end distance to contour length. Lower ratio indicates more curved filaments. **(D)** Liposome flotation assays showing very limited membrane binding of CdvB2ΔC alone. **(E)** Microscopy image of fluorescently labelled CdvB2ΔC reconstituted inside dumbbell-shaped liposomes and localizing at necks. **(F)** Liposome flotation assays showing clear membrane binding of CdvB1 alone. **(G)** Microscopy image of fluorescently labelled CdvB1 reconstituted inside dumbbell-shaped liposomes and localizing at necks. **(H)** Liposome flotation assays showing CdvB2ΔC being recruited to membranes along with CdvB1. **(I)** Microscopy image of a fluorescently labelled CdvB1:CdvB2ΔC complex reconstituted inside dumbbell-shaped liposomes and localizing at necks.

CdvB1 and CdvB2ΔC binding to membrane necks

Subsequently, we tested the ability of CdvB2ΔC to bind lipid membranes. When mixed with negatively charged SUVs, CdvB2ΔC was almost exclusively found in the soluble and filamented fractions (**Figure 2D** [↗](#)), with only a small fraction of the protein found in the lipid-bound fraction. In spite of its low affinity, we encapsulated CdvB2ΔC in dumbbells using the SMS technique and observed instances of CdvB2ΔC clusters at their neck (**Figure 2E** [↗](#)). It is possible that, in the presence of the correct membrane curvature found at the neck of dumbbells, the affinity of CdvB2ΔC for membrane may increase, indicating that CdvB2ΔC is able to sense curvature. CdvB1 presented clear membrane binding when mixed with liposomes on its own (**Figure 2F** [↗](#)), as we previously showed ([Blanch Jover et al., 2022](#) [↗](#)). CdvB1 also exhibited preferential neck localization when reconstituted in dumbbells (**Figure 2G** [↗](#)). When mixing the two proteins and subsequently adding them to SUVs, CdvB1 appears to recruit CdvB2ΔC to the membrane (**Figure 2H** [↗](#)), indicating that they form a complex. Accordingly, we observe binding of the CdvB1:CdvB2ΔC complex to the neck of dumbbell liposomes (**Figure 2I** [↗](#)).

Reconstitution of a quaternary

CdvA:CdvB:CdvB1:CdvB2ΔC complex at a membrane neck

Finally, we explored the interaction between the CdvA:CdvB and CdvB1:CdvB2ΔC complexes in the presence of lipid membranes. In flotation assays, CdvB1 was recruited to the membrane in the presence of CdvA and CdvB (**Figure 3A** [↗](#) and Supplementary Figure 3A). Moreover, the CdvA:CdvB complex was also able to recruit CdvB2ΔC to liposomes (**Figure 3A** [↗](#)). Finally, when mixing all four proteins together in the presence of liposomes, we observed that they were all recruited to liposomes (**Figure 3A** [↗](#) and Supplementary Figure 3B). Thus, our data indicate that either CdvB1 or a CdvA:CdvB complex (or both) can recruit CdvB2 to the membrane.

We then reconstituted the same combinations of Cdv proteins inside dumbbells-shaped liposomes: CdvA (unlabelled) + CdvB + CdvB1 (**Figure 3B** [↗](#)); CdvA (unlabelled) + CdvB + CdvB2ΔC (**Figure 3C** [↗](#)) and CdvA (unlabelled) + CdvB + CdvB1 + CdvB2ΔC (**Figure 3D** [↗](#)). In passing we note that assembly of such a quaternary Cdv complex at membrane necks of dumbbell-shaped liposomes resembling the shape of a dividing cell has never been achieved before. In all cases, we observed a clear preference of the complexes to assemble onto regions of high membrane curvature, as demonstrated by the strong fluorescence signal at the membrane necks. In the quaternary complex, the fluorescence intensity of the Cdv proteins at the necks was about 7 times higher than that at the membrane away from the necks. For comparison, the lipid fluorescence intensity at the neck was only ~2 times enhanced (Supplementary Figure 3C) as expected in the neck region where the membrane of the two lobes are in close proximity.

Discussion

In this study, we elucidated the protein interaction network that governs Cdv protein assembly at the membrane, and showed that Cdv complexes spontaneously localize at membrane necks. We learned that full-length CdvA can form filaments without the need of DNA to stabilize them, but that it does not bind membranes on its own. However, while CdvB by itself is also unable to bind membranes ([Samson et al., 2011](#) [↗](#)), the CdvA:CdvB complex efficiently binds the membrane. This suggests that both proteins are likely recruited to the membrane jointly. We confirmed our previous finding that CdvB1 interacts with membranes on its own ([Blanch Jover et al., 2022](#) [↗](#)). Furthermore, we purified CdvB2 and showed that it is able to polymerize into filaments once the C-terminal domain is removed. This is a relevant parallelism with the ESCRT machinery, where many of the proteins also only polymerize upon removal of the C-terminus. We observed that CdvB2 binds poorly the membrane by itself, even upon removal of the C-terminal. However, we

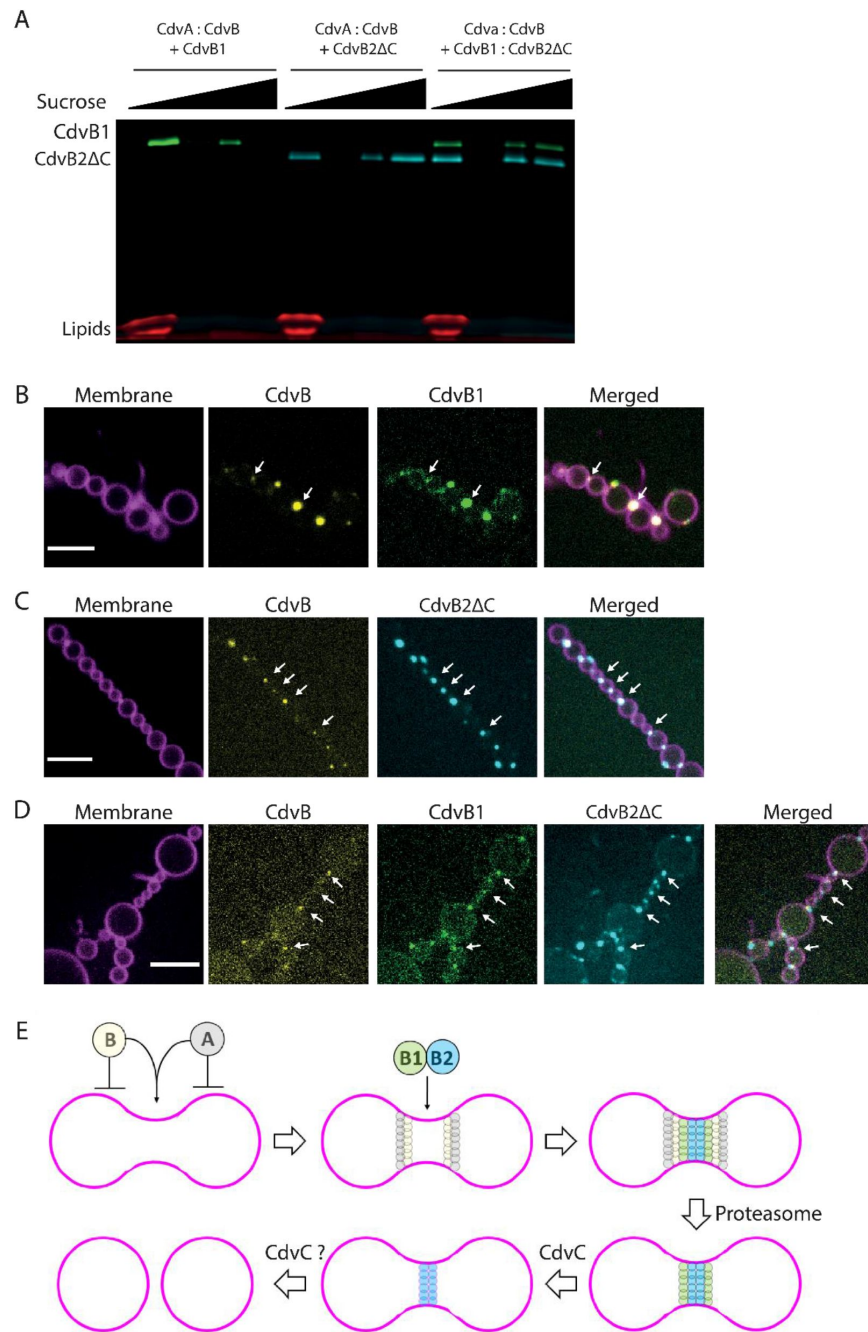


Figure 3.

membrane binding of the CdvA:CdvB:CdvB1:CdvB2ΔC quaternary complex

(A) Liposome flotation assays showing recruitment of CdvB1 and CdvB2ΔC to membranes, either alone or in combination, by the CdvA:CdvB complex. **(B)** Spinning disk confocal images of the ternary complex CdvA (unlabelled) + CdvB-Alexa568 + CdvB1-Alexa488 reconstituted inside the neck of dumbbell liposomes. **(C)** Spinning disk confocal images of the ternary complex CdvA (unlabelled) + CdvB-Alexa568 + CdvB2ΔC-Cy5 reconstituted inside the neck of dumbbell liposomes. **(D)** Spinning disk confocal images of the quaternary complex CdvA (unlabelled) + CdvB-Alexa568 + CdvB1-Alexa488 + CdvB2ΔC-Cy5 reconstituted inside the neck of dumbbell liposomes. Scale bars: 10 μm. **(E)** Schematic depicting the stepwise assembly and disassembly of the Cdv division ring. CdvA and CdvB cannot bind the membrane individually, but they are able to assemble at the neck by forming a complex. Once the CdvA:CdvB ring is assembled, CdvB1 and CdvB2 are both recruited at the neck. Subsequently, the proteasome removes CdvA, and CdvC removes CdvB1, leaving only CdvB2, which may be removed by CdvC, thus achieving membrane abscission.

observed that either CdvB1 or a CdvA:CdvB complex (or both) can recruit CdvB2 Δ C to the membrane, which suggests that CdvB2 Δ C interaction with the membrane may be indirect. Intriguingly however, we also observe binding of CdvB2 Δ C alone to highly curved membrane, which is the geometry found at the neck of dumbbells. Thus, it is also possible that the mechanism by which CdvB1 and the CdvA:CdvB complex recruit CdvB2 Δ C at the membrane is by generating curvature. Further work is needed to thoroughly dissect this phenomenon for the various Cdv proteins.

Recently, *in vivo* imaging showed that CdvB1 is required to facilitate the spatial separation of CdvB and CdvB2 polymers, as absence of CdvB1 caused a spatial overlapping of CdvB and CdvB2 polymers at the intercellular bridge of dividing cells (Hurtig et al., 2023 [↗](#)). Our *in vitro* data show that indeed CdvB2 can be recruited to the membrane by the CdvA:CdvB complex even in the absence of CdvB1. This suggests that the co-localization of CdvB and CdvB2 in the absence of CdvB1 *in vivo* is likely driven by direct interaction between CdvB and CdvB2.

Moreover, in simulations it was observed that, to obtain a non-overlapping arrangement of Cdv polymers, CdvB1 filaments should be relatively flexible compared to both CdvB and CdvB2 filaments (Hurtig et al., 2023 [↗](#)). Our *in vitro* data are consistent with this scenario, as we observe that the CdvB1:CdvB2 co-polymers are more curved, and thus potentially more flexible, than the CdvB2 homo-polymers.

We found that all Cdv proteins preferentially localize at membrane necks, providing the first experimental evidence of affinity of Cdv proteins for high-curvature membranes. This presents another common trait between the archaeal and eukaryotic systems, as many ESCRT proteins also preferentially bind highly curved membranes (Lee et al., 2015 [↗](#); De Franceschi et al., 2018 [↗](#); Bertin et al., 2020 [↗](#); Pfitzner et al., 2020 [↗](#)). Using super-resolution microscopy, it was shown that Cdv proteins arrange in ring-like structures that are not completely overlapping; that is, they take distinct spatial positions within the relatively highly curved membrane of the division ring (Hurtig et al., 2023 [↗](#)). Our system is currently only amenable for standard confocal microscopy, due to constant moving of the dumbbells (De Franceschi et al., 2022 [↗](#)). However, we can envision that protocols for fixation of dumbbells can be developed in the future, which would allow to investigate the assembly of recombinant proteins at the neck region using super-resolution microscopy.

Based on both literature and our own data, we can propose an updated model for the hierarchical assembly of Cdv proteins regulated by protein-protein interactions (**Figure 3E** [↗](#)): Initially, CdvA and CdvB are recruited to the neck via their mutual interaction. Once the CdvA:CdvB complex forms a ring at the membrane, CdvB1 and CdvB2 are also recruited. In our experiment, CdvB1 and CdvB2 can bind the neck even in the absence of a pre-existing CdvA:CdvB complex at the membrane. However, the SMS system itself generates curvature (De Franceschi et al., 2022 [↗](#)) and this may favour membrane binding, as our data suggest in the case of CdvB2. *In vivo*, recruitment of CdvB1 and CdvB2 may not occur unless a CdvA:CdvB complex is present. In all our experiments, we observe that CdvB1 and CdvB2 Δ C always form a complex, whether in the presence of a membrane or not. Thus is it reasonable to assume that they are also recruited to the CdvA:CdvB complex together. Once the quaternary complex is assembled, CdvB is removed by the proteasome (Tarrason, 2020). In this regard, we provide the crucial piece of evidence that the CdvB1:CdvB2 complex can bind to membrane necks independently of the CdvA:CdvB complex. CdvB1 is subsequently removed from the membrane by CdvC (Blach-Jover, 2022), and here we show that CdvB2 can also bind to membrane necks by itself, without the presence of CdvB1.

We positioned the different subunits in our schematics (**Figure 3E** [↗](#)) based on their preferred radius of curvature proposed in (Hurtig et al., 2023 [↗](#)), obtaining a final arrangement that resembles the later stage of constriction reported in (Hurtig et al., 2023 [↗](#)). We expect this arrangement to be the case in our reconstituted system, even though the Cdv proteins are added

simultaneously, because the shape of a neck is provided by the SMS system itself (De Franceschi et al., 2022 [↗](#)) and therefore each protein can bind to the region having its preferred radius of curvature. This reconstituted system sets the stage to test Cdv-mediated membrane scission in the future, and in particular disassembly of CdvB1 and CdvB2 polymers from membrane necks by the action of CdvC. This will require the use of a sulfoscope (Pulschen et al., 2020 [↗](#)), i.e., a microscope working at elevated temperatures, given that the catalytic activity of CdvC requires high temperature (Blanch Jover et al., 2022 [↗](#)).

Methods

Plasmids

All of the proteins that we used are from *Metallosphaera sedula*. The original plasmids for CdvA (Msed_1670, UniProtID A4YHC3) and CdvB (Msed_1671, UniProtID A4YHC4) were kindly provided to us by Patricia Renesto's lab. From those plasmids, the sequences of the proteins were copied and ordered as a synthetic gene already inserted in a pMAL-c5x from Biomatik, using BamHI and EcoRI cutting sites. Extra codons coding for cysteines were added at the N termini of the proteins for fluorescent labelling. The plasmid for CdvB1 was the same as used in our previous work (8). The gene for CdvB2 (Msed_1695, UniProtID A4YHE8) was obtained from the Gen Bank data base, and was reverse translated using the EMBOSS Backtranseq tool, optimized for *E. coli* codon usage. To the resulting DNA sequence, a codon of a cysteine for fluorescent labelling was added at the N terminal of the protein, as well as Tobacco Etch Virus (TEV) and an HRV 3C proteases cutting sites. The whole gene construct was ordered as a synthetic gene already inserted in a pMAL-c5x vector from Biomatik, using BamHI and EcoRI cutting sites.

From the original plasmid for MBP-CdvB2, the whole plasmid except for the C-terminus of the protein was copied by PCR. The resulting linearized plasmid was checked on an agarose gel, and then treated with the KLD reaction mix (New England Biolabs, Ipswich, Massachusetts, USA) to digest the template, phosphorylate the ends of the linearized plasmid and ligate it all at once. The reaction mix was then transformed into NEB5alpha competent cells (New England Biolabs), some colonies were picked, and the plasmid was purified using the QIAprep Spin Miniprep Kit (QIAGEN, Hilden, Germany) and sent for sequencing.

4.4.2. Protein purification

All proteins were produced in BL-21 *E. coli* strains. Cells were grown at 37°C in LB^{amp} medium to an OD of around 0.5, at which point expression was induced with IPTG and cells were left to express the protein for 4 hours. After that, cells were harvested by centrifuging at 4500x g at 4°C for 12 minutes. For MBP-CdvA, the cell pellet was resuspended in lysis buffer (50mM Tris pH 8.8, 350 mM NaCl, 50 mM Glutamate, 50 mM Arginine, 0.05mM TCEP, cComplete™ Protease Inhibitor Cocktail (Roche, Basel, Switzerland)), lysed by French press and centrifuged (150,000 g, 30 min, 4°C). The remaining supernatant was incubated with 1 ml of amylose resin (NEB, Ipswich, Massachusetts, USA) rotating for 2 hours at 4°C, after which it was poured through a gravity chromatography column and the protein was washed (50 mM Tris pH 8.8, 350 mM NaCl, 50 mM Glutamate, 50 mM Arginine, 0.05 mM TCEP) and eluted with elution buffer (50 mM Tris pH 8.8, 350 mM NaCl, 50 mM Glutamate, 50 mM Arginine, 0.05 mM TCEP, 10 mM maltose). For MBP-CdvB, MBP-CdvB2 and MBP-CdvB2ΔC, the cell pellet was resuspended in lysis buffer (50mM

Tris pH 8.8, 50 mM NaCl, 0.05 mM TCEP, cComplete™ Protease Inhibitor Cocktail) lysed by French press and centrifuged (150,000 g, 30 min, 4°C). The remaining supernatant was incubated with 1ml of amylose resin rotating for 2 hours at 4°C, after which it was poured through a gravity chromatography column and the protein was washed (50 mM Tris pH 8.8, 50 mM NaCl, 0.05 mM TCEP) eluted with elution buffer (50 mM Tris pH 8.8, 50 mM NaCl, 0.05 mM TCEP, 10 mM maltose).

MBP-CdvB1 was purified just as described in (8). After affinity chromatography, all proteins were run through a Superdex™ 75 increase 10/300 GL size exclusion chromatography column mounted in an ÄKTA™ Pure system. Samples were run with the same buffer as they were washed and stored by snap freeze in liquid nitrogen. Purity of the samples was evaluated by SDS PAGE stained with Coomassie blue. A fraction of all of the proteins was separated after the affinity chromatography and dialyzed into the same buffer but with pH of 7.4 to perform a maleimide-cysteine conjugation reaction. MBP-CdvA was labelled with Cy5, MBP-CdvB with Alexa-568, MBP-CdvB2ΔC with Cy5 and CdvB1 with Alexa 488. The rest of the purification stayed the same, and excess label was removed from the protein through the gel filtration column.

4.4.3. TEM imaging

For imaging of MBP-CdvA, the protein was diluted down to 100 nM in buffer containing 50 mM Tris pH 7.4 and 50 mM NaCl (all samples were prepared using this buffer). For imaging the protein without MBP, 1 μM of MBP-CdvA was mixed with 0.1 μM of TEV protease and left incubating at RT for 1 hour. The sample was then diluted 10 times before depositing it onto a carbon grid. MBP-CdvB2ΔC samples were diluted down to 100 nM in buffer, and samples without MBP were prepared by mixing 1 μM of MBP-CdvB2ΔC with 0.1 μM of TEV protease and left incubating at RT for 1 hour. Samples with CdvB1 and CdvB2ΔC were prepared by mixing MBP-CdvB1 and MBP-CdvB2ΔC both at 1 μM concentration with 0.1 μM of TEV protease at RT for 1 hour. The samples were then diluted 10 times before depositing it onto a carbon grid. Samples were absorbed on glow-discharged carbon-coated 400-mesh copper grid purchased from Quantifoil (Großlöbichau, Germany) and stained with 2 % uranyl acetate. They were then imaged on a JEOL JEM-1400plus TEM (JEOL, Akishima, Tokyo, Japan) at 120 kV of accelerating voltage with a TVIPS f416 camera (TVIPS, Gauting, Germany).

4.4.4. Liposome flotation assay

Lipids used were DOPC (1,2-dioleoyl-sn-glycero-3-phosphocholine), DOPG (1,2-dioleoyl-sn-glycero-3-phospho-(1'-rac-glycerol)), and Rhodamine-PE (1,2-dioleoyl-sn-glycero-3-phosphoethanolamine-N-(lissamine rhodamine B sulfonyl)), all of them purchased from Avanti Polar Lipids (Alabaster, Alabama, USA). The lipids, dissolved in chloroform, were mixed to final ratios (mol:mol) of 69.9 DOPC : 30 DOPG : 0.1 Rhodamine-PE, and evaporated in a glass vial to obtain a thin lipid film. Lipids were resuspended in buffer containing 50 mM HEPES pH 7.5, 50 mM NaCl and 300 mM sucrose, at a final concentration of 5 mg/ml. The lipid film was hydrated for 1 hour and thoroughly vortexed and sonicated to form SUVs. The lipids were then mixed with 0.1 μM of TEV protease and 1 μM of protein of interest. Lipids and protein were left to incubate for 1 hour at RT. The sample was then deposited at the bottom of an ultracentrifuge tube, and mixed with buffer containing sucrose to obtain a bottom layer of 30% of sucrose. Gently, another layer of buffer with 25% of sucrose was deposited, and a final layer of 0% of sucrose on top. Then it was centrifuged at 200,000 g at 4 °C for 30 minutes in a SW 60 Ti Swinging Bucket rotor. All the different fractions of the sucrose gradient were then pipetted out and extra buffer was then added to resuspend the filamented pellet at the bottom. The different fractions were then analysed by SDS PAGE, and stained with Coomassie blue. Experiments with CdvB2ΔC were done with a final concentration of all the proteins of 600nM, and gels were imaged using a GE Amersham™ Typhoon gel imager to image the fluorescent label on the proteins and lipids.

4.4.5. Preparation of lipid in oil suspension for dumbbell-shaped liposome preparations

DOPC, DOPE-PEG2000, DOPG and DOPE-Rhodamine (or DOPE-Atto390 for experiments with proteins with overlapping fluorescence) in chloroform were mixed in a ratio of 93:2:5:0.1 and evaporated in a glass vial under a blow of nitrogen. Lipid mixture was then resolubilized in chloroform to a final concentration of 0.2 mg/ml. A freshly prepared mixture of silicone and

mineral oil that was added to the lipids in chloroform slowly dropwise while vortexing gently. After all oil is added to the chloroform, it was vortexed at max speed for 2 minutes and then sonicated for 15 minutes in an ice bath.

4.4.6. Preparation of dumbbell-shaped liposomes with the synthetic membrane shaper

Cdv proteins were mixed in an inner buffer containing 50mM Tris pH 7.5 and 37 % w/v optiprep (Sigma Aldrich, St. Louis, Missouri, USA) to make the solution heavy. In parallel, an outer solution in buffer containing 50 mM Tris pH7.4, 5 mM MgCl₂ and glucose to match the osmolarity of the outer solution at 30 mOsm higher than in the inner solution. The DNA nanostars developed in Ref. (24) were then mixed into the outer solution and deposited at the bottom of an imaging chamber. Water in oil droplets of inner buffer containing protein were then formed by pipetting up and down 20 µl of inner solution into 400 µl of oil until a homogeneous droplet size was achieved. The droplets in oil were immediately deposited on top of the outer solution in the imaging chamber, and they were allowed to sediment by gravity through the oil-water interphase. The liposomes were imaged using spinning disk confocal laser microscopy (Olympus IXB1/BX61 microscope, 60× objective, iXon camera) with Andor iQ3 software. Analysis of the images was done with ImageJ (v.2.1.0).

Acknowledgements

We Eli van der Sluis and Ashmiani van den Berg for discussions and protein purification. We acknowledge funding support from the BaSyC program of NWO-OCW, from the ERC Advanced Grant 883684, and from the NCN Polonez Bis grant 2022/45/P/NZ1/01565.

Additional files

Supplementary Figures 1,2,3 [↗](#)

References

- Azad K *et al.* (2023) **Structural basis of CHMP2A-CHMP3 ESCRT-III polymer assembly and membrane cleavage** *Nat Struct Mol Biol* **30**:81–90
- Bertin A *et al.* (2020) **Human ESCRT-III polymers assemble on positively curved membranes and induce helical membrane tube formation** *Nat Commun* **11**
- Blanch Jover A, De Franceschi N, Fenel D, Weissenhorn W, Dekker C. (2022) **The archaeal division protein CdvB1 assembles into polymers that are depolymerized by CdvC** *FEBS Lett* **596**:958–969
- Caillat C, Macheboeuf P, Wu Y, McCarthy AA, Boeri-Erba E, Effantin G, Göttlinger HG, Weissenhorn W, Renesto P. (2015) **Asymmetric ring structure of Vps4 required for ESCRT-III disassembly** *Nat Commun* **6**
- Caspi Y, Dekker C. (2018) **Dividing the Archaeal Way: The Ancient Cdv Cell-Division Machinery** *Front Microbiol* **9**
- Chiaruttini N, Redondo-Morata L, Colom A, Humbert F, Lenz M, Scheuring S, Roux A. (2015) **Relaxation of Loaded ESCRT-III Spiral Springs Drives Membrane Deformation** *Cell* **163**:866–79
- Cox CJ, Foster PG, Hirt RP, Harris SR, Embley TM (2008) **The archaeobacterial origin of eukaryotes** *Proc Natl Acad Sci U S A* **105**:20356–61
- De Franceschi N, Alqabandi M, Miguet N, Caillat C, Mangenot S, Weissenhorn W, Bassereau P. (2018) **The ESCRT protein CHMP2B acts as a diffusion barrier on reconstituted membrane necks** *J Cell Sci* **132**
- De Franceschi N, Barth R, Meindlhumer S, Fragasso A, Dekker C. (2024) **Dynamain A as a one-component division machinery for synthetic cells** *Nat Nanotechnol* **19**:70–76
- De Franceschi N, Pezeshkian W, Fragasso A, Bruininks BMH, Tsai S, Marrink SJ, Dekker C. (2022) **Synthetic Membrane Shaper for Controlled Liposome Deformation** *ACS Nano* **17**:966–78
- Dobro MJ, Samson RY, Yu Z, McCullough J, Ding HJ, Chong PL, Bell SD, Jensen GJ (2013) **Electron cryotomography of ESCRT assemblies and dividing Sulfolobus cells suggests that spiraling filaments are involved in membrane scission** *Mol Biol Cell* **24**:2319–27
- Harker-Kirschneck L *et al.* (2022) **Physical mechanisms of ESCRT-III-driven cell division** *Proc Natl Acad Sci U S A* **119**
- Hurley JH (2015) **ESCRTs are everywhere** *EMBO J* **34**:2398–407
- Hurtig F *et al.* (2023) **The patterned assembly and stepwise Vps4-mediated disassembly of composite ESCRT-III polymers drives archaeal cell division** *Sci Adv* **9**
- Lata S, Schoehn G, Jain A, Pires R, Piehler J, Gottlinger HG, Weissenhorn W. (2008) **Helical structures of ESCRT-III are disassembled by VPS4** *Science* **321**:1354–7

- Lee IH, Kai H, Carlson LA, Groves JT, Hurley JH (2015) **Negative membrane curvature catalyzes nucleation of endosomal sorting complex required for transport (ESCRT)-III assembly** *Proc Natl Acad Sci U S A* **112**:15892–7
- Lindås AC, Karlsson EA, Lindgren MT, Ettema TJ, Bernander R. (2008) **A unique cell division machinery in the Archaea** *Proc Natl Acad Sci U S A* **105**:18942–6
- Makarova KS, Yutin N, Bell SD, Koonin EV (2010) **Evolution of diverse cell division and vesicle formation systems in Archaea** *Nat Rev Microbiol* **8**:731–41
- Moriscot C, Gribaldo S, Jault JM, Krupovic M, Arnaud J, Jamin M, Schoehn G, Forterre P, Weissenhorn W, Renesto P. (2011) **Crenarchaeal CdvA forms double-helical filaments containing DNA and interacts with ESCRT-III-like CdvB** *PLoS One* **6**
- Pfützner AK, Mercier V, Jiang X, Moser von Filseck J, Baum B, Šarić A, Roux A. (2020) **An ESCRT-III Polymerization Sequence Drives Membrane Deformation and Fission** *Cell* **182**:1140–1155
- Pulschen AA *et al.* (2020) **Live Imaging of a Hyperthermophilic Archaeon Reveals Distinct Roles for Two ESCRT-III Homologs in Ensuring a Robust and Symmetric Division** *Curr Biol* **30**:2852–2859
- Samson RY, Obita T, Freund SM, Williams RL, Bell SD (2008) **A role for the ESCRT system in cell division in archaea** *Science* **322**:1710–3
- Samson RY, Obita T, Hodgson B, Shaw MK, Chong PL, Williams RL, Bell SD (2011) **Molecular and structural basis of ESCRT-III recruitment to membranes during archaeal cell division** *Mol Cell* **41**:186–96
- Shim S, Kimpler LA, Hanson PI (2007) **Structure/function analysis of four core ESCRT-III proteins reveals common regulatory role for extreme C-terminal domain** *Traffic* **8**:1068–79
- Schöneberg J, Lee IH, Iwasa JH, Hurley JH (2017) **Reverse-topology membrane scission by the ESCRT proteins** *Nat Rev Mol Cell Biol* **18**:5–17
- Tang S, Henne WM, Borbat PP, Buchkovich NJ, Freed JH, Mao Y, Fromme JC, Emr SD (2015) **Structural basis for activation, assembly and membrane binding of ESCRT-III Snf7 filaments** *Elife* **4**
- Tarrason Risa G *et al.* (2020) **The proteasome controls ESCRT-III-mediated cell division in an archaeon** *Science* **369**

Author information

Nicola De Franceschi[#]

Department of Bionanoscience, Kavli Institute of Nanoscience Delft, Delft University of Technology, Delft, The Netherlands, IMol Polish Academy of Sciences, Warsaw, Poland
ORCID iD: [0000-0002-7221-613X](https://orcid.org/0000-0002-7221-613X)

[#]equal contribution

Alberto Blanch-Jover[#]

Department of Bionanoscience, Kavli Institute of Nanoscience Delft, Delft University of Technology, Delft, The Netherlands

ORCID iD: [0000-0002-1484-7793](https://orcid.org/0000-0002-1484-7793)

[#]equal contribution

Cees Dekker

Department of Bionanoscience, Kavli Institute of Nanoscience Delft, Delft University of Technology, Delft, The Netherlands

ORCID iD: [0000-0001-6273-071X](https://orcid.org/0000-0001-6273-071X)

For correspondence: C.Dekker@tudelft.nl

Editors

Reviewing Editor

Felix Campelo

Institute of Photonic Sciences, Barcelona, Spain

Senior Editor

Felix Campelo

Institute of Photonic Sciences, Barcelona, Spain

Reviewer #1 (Public review):

Summary:

The authors aimed to elucidate the recruitment order and assembly of the Cdv proteins during *Sulfolobus acidocaldarius* archaeal cell division using a bottom-up reconstitution approach. They employed liposome-binding assays, EM, and fluorescence microscopy with *in vitro* reconstitution in dumbbell-shaped liposomes to explore how CdvA, CdvB, and the homologues of ESCRT-III proteins (CdvB, CdvB1, and CdvB2) interact to form membrane remodeling complexes.

The study sought to reconstitute the Cdv machinery by first analyzing their assembly as two sub-complexes: CdvA:CdvB and CdvB1:CdvB2ΔC. The authors report that CdvA binds lipid membranes only in the presence of CdvB and localizes preferentially to membrane necks. Similarly, the findings on CdvB1:CdvB2ΔC indicate that truncation of CdvB2 facilitates filament formation and enhances curvature sensitivity in interaction with CdvB1. Finally, while the authors reconstitute a quaternary CdvA:CdvB:CdvB1:CdvB2 complex and demonstrate its enrichment at membrane necks, the mechanistic details of how these complexes drive membrane remodeling by subcomplexes removal by the proteasome and/or CdvC remain speculative.

Although the work highlights intriguing similarities with eukaryotic ESCRT-III systems and explores unique archaeal adaptations, the conclusions drawn would benefit from stronger experimental validation and a more comprehensive mechanistic framework.

Strengths:

The study of machinery assembly and its involvement in membrane remodeling, particularly using bottom-up reconstituted *in vitro* systems, presents significant challenges. This is particularly true for systems like the ESCRT-III complex, which localizes uniquely at the lumen of membrane necks prior to scission. The use of dumbbell-shaped liposomes in this

study provides a promising experimental model to investigate ESCRT-III and ESCRT-III-like protein activity at membrane necks.

The authors present intriguing evidence regarding the sequential recruitment of ESCRT-III proteins in crenarchaea—a close relative of eukaryotes. This finding suggests that the hierarchical recruitment characteristic of eukaryotic systems may predate eukaryogenesis, which is a significant and exciting contribution. However, the broader implications of these findings for membrane remodeling mechanisms remain speculative, and the study would benefit from stronger experimental validation and expanded contextualization within the field.

Weaknesses:

This manuscript presents several methodological inconsistencies and lacks key controls to validate its claims. Additionally, there is insufficient information about the number of experimental repetitions, statistical analyses, and a broader discussion of the major findings in the context of open questions in the field.

<https://doi.org/10.7554/eLife.104226.1.sa3>

Reviewer #2 (Public review):

Summary:

The Crenarchaeal Cdv division system represents a reduced form of the universal and ubiquitous ESCRT membrane reverse-topology scission machinery, and therefore a prime candidate for synthetic and reconstitution studies. The work here represents a solid extension of previous work in the field, clarifying the order of recruitment of Cdv proteins to curved membranes.

Strengths:

The use of a recently developed approach to produce dumbbell-shaped liposomes (De Franceschi et al. 2022), which allowed the authors to assess recruitment of various Cdv assemblies to curved membranes or membrane necks; reconstitution of a quaternary Cdv complex at a membrane neck.

Weaknesses:

The manuscript is a bit light on quantitative detail, across the various figures, and several key controls are missing (CdvA, B alone to better interpret the co-polymerisation phenotypes and establish the true order of recruitment, for example) - addressing this would make the paper much stronger. The authors could also include in the discussion a short paragraph on implications for our understanding of ESCRT function in other contexts and/or in archaeal evolution, as well as a brief exploration of the possible reasons for the discrepancy between the foci observed in their liposome assays and the large rings observed in cells - to better serve the interests of a broad audience.

<https://doi.org/10.7554/eLife.104226.1.sa2>

Reviewer #3 (Public review):

Summary:

In this report, De Franceschi et al. purify components of the Cdv machinery in archaeon *M. sedula* and probe their interactions with membrane and with one-another in vitro using two

main assays - liposome flotation and fluorescent imaging of encapsulated proteins. This has the potential to add to the field by showing how the order of protein recruitment seen in cells is related to the differential capacity of individual proteins to bind membranes when alone or when combined.

Strengths:

Using the floatation assay, they demonstrate that CdvA and CdvB bind liposomes when combined. While CdvB1 also binds liposomes under these conditions, in the floatation assay, CdvB2 lacking its C-terminus is not efficiently recruited to membranes unless CdvAB or CdvB1 are present. The authors then employ a clever liposome assay that generates chained spherical liposomes connected by thin membrane necks, which allows them to accurately control the buffer composition inside and outside of the liposome. With this, they show that all four proteins accumulate in necks of dumbbell-shaped liposomes that mimic the shape of constricting necks in cell division. Taken altogether, these data lead them to propose that Cdv proteins are sequentially recruited to the membrane as has also been suggested by *in vivo* studies of ESCRT-III dependent cell division in crenarchaea.

Weaknesses:

These experiments provide a good starting point for the *in vitro* study the interaction of Cdv system components with the membrane and their consecutive recruitment. However, several experimental controls are missing that complicate their ability to draw strong conclusions. Moreover, some results are inconsistent across the two main assays which make the findings difficult to interpret.

(1) Missing controls.

Various protein mixtures are assessed for their membrane-binding properties in different ways. However, it is difficult to interpret the effect of any specific protein combination, when the same experiment is not presented in a way that includes separate tests for all individual components. In this sense, the paper lacks important controls.

For example, Fig 1C is missing the CdvB-only control. The authors remark that CdvB did not polymerise (data not shown) but do not comment on whether it binds membrane in their assays. In the introduction, Samson et al., 2011 is cited as a reference to show that CdvB does not bind membrane. However, here the authors are working with protein from a different organism in a different buffer, using a different membrane composition and a different assay. Given that so many variables are changing, it would be good to present how *M. sedula* CdvB behaves under these conditions.

Similarly, there is no data showing how CdvB alone or CdvA alone behave in the dumbbell liposome assay. Without these controls, it's impossible to say whether CdvA recruits CdvB or the other way around.

The manuscript would be much stronger if such data could be added.

(2) Some of the discrepancies in the data generated using different assays are not discussed.

The authors show that CdvB2 Δ C binds membrane and localizes to membrane necks in the dumbbell liposome assay, but no membrane binding is detected in the flotation assay. The discrepancy between these results further highlights the need for CdvB-only and CdvA-only controls.

(3) Validation of the liposome assay.

The experimental setup to create dumbbell-shaped liposomes seems great and is a clever novel approach pioneered by the team. Not only can the authors manipulate liposome shape,

they also state that this allows them to accurately control the species present on the inside and outside of the liposome. Interpreting the results of the liposome assay, however, depends on the geometry being correct. To make this clearer, it would seem important to include controls to prove that all the protein imaged at membrane necks lie on the inside of liposomes. In the images in SFig3 there appears to be protein outside of the liposome. It would also be helpful to present data to show test whether the necks are open, as suggested in the paper, by using FRAP or some other related technique.

(4) Quantification of results from the liposome assay.

The paper would be strengthened by the inclusion of more quantitative data relating to the liposome assay. Firstly, only a single field of view is shown for each condition. Because of this, the reader cannot know whether this is a representative image, or an outlier? Can the authors do some quantification of the data to demonstrate this? The line scan profiles in the supplemental figures would be an example of this, but again in these Figures only a single image is analyzed.

We would recommend that the authors present quantitative data to show the extent of colocalization at the necks in each case. They also need a metric to report instances in which protein is not seen at the neck, e.g. CdvB2 but not CdvB1 in Fig2I, which rules out a simple curvature preference for CdvB2 as stated in line 182.

Secondly, the authors state that they see CdvB2 Δ C recruited to the membrane by CdvB1 (lines 184-187, Fig 2I). However, this simple conclusion is not borne out in the data. Inspecting the CdvB2 Δ C panels of Fig 2I, Fig3C, and Fig3D, CdvB2 Δ C signal can be seen at positions which don't colocalize with other proteins. The authors also observe CdvB2 Δ C localizing to membrane necks by itself (Fig 2E). Therefore, while CdvB1 and CdvB2 Δ C colocalize in the flotation assay, there is no strong evidence for CdvB2 Δ C recruitment by CdvB1 in dumbbells. This is further underscored by the observation that in the presented data, all Cdv proteins always appear to localize at dumbbell necks, irrespective of what other components are present inside the liposome. Although one nice control is presented (ZipA), this suggests that more work is required to be sure that the proteins are behaving properly in this assay. For example, if membrane binding surfaces of Cdv proteins are mutated, does this lead to the accumulation of proteins in the bulk of the liposome as expected?

(5) Rings.

The authors should comment on why they never observe large Cdv rings in their experiments. In crenarchaeal cell division, CdvA and CdvB have been observed to form large rings in the middle of the 1 micron cell, before constriction. Only in the later stages of division are the ESCRTs localized to the constricting neck, at a time when CdvA is no longer present in the ring. Therefore, if the *in vitro* assay used by the authors really recapitulated the biology, one would expect to see large CdvAB rings in Figs 1EF. This is ignored in the model. In the proposed model of ring assembly (line 252), CdvAB ring formation is mentioned, but authors do not discuss the fact that they do not observe CdvAB rings - only foci at membrane necks. The discussion section would benefit from the authors commenting on this.

(6) Stoichiometry

It is not clear why 100% of the visible CdvA and 100% of the the visible CdvB are shifted to the lipid fraction in 1C. Perhaps this is a matter of quantification. Can the authors comment on the stoichiometry here?

(7) Significance of quantification of MBP-tagged filaments.

Authors use tagging and removal of MBP as a convenient, controllable system to trigger polymerisation of various Cdv proteins. However, it is unclear what is the value and significance of reporting the width and length of the short linear filaments that are formed by the MBP-tagged proteins. Presumably they are artefactual assemblies generated by the presence of the tag? Similar Figure 2C doesn't seem a useful addition to the paper.

<https://doi.org/10.7554/eLife.104226.1.sa1>

Author response:

We thank the three Reviewers for the extensive evaluation of our work, which was largely positive and constructive. Prompted by their reviews and the many suggestions, we plan to do additional control experiments to add further data in a revised manuscript in order to improve the statistics and quantitation. Furthermore, we plan to expand the discussion. We agree that a more comprehensive mechanistic framework would be welcome but note that the system is a complex multicomponent system which is challenging. We plan to expand the work in future follow-up research.

<https://doi.org/10.7554/eLife.104226.1.sa0>